

The Effect of Rapid Maxillary Expansion on the Upper Airway's Aerodynamic Characteristics

Xin Feng

University of Bergen

Yicheng Chen

Harbin Institute of Technology

Kristina Halme

Malmö University

Weihua Cai

Northeast Electric Power University

Xie-Qi Shi (✉ xieqi.shi@uib.no)

University of Bergen

Research Article

Keywords: Computational fluid dynamics, Upper airway, Adenoid hypertrophy, Rapid maxillary expansion

Posted Date: December 21st, 2020

DOI: <https://doi.org/10.21203/rs.3.rs-129339/v1>

License: © ⓘ This work is licensed under a Creative Commons Attribution 4.0 International License. [Read Full License](#)

Version of Record: A version of this preprint was published on March 17th, 2021. See the published version at <https://doi.org/10.1186/s12903-021-01488-1>.

Abstract

Background: The effect of rapid maxillary expansion (RME) on the upper airway (UA) has been studied earlier but without a consistent conclusion. This study aims to evaluate the outcome of RME on the upper airway function in terms of airflow resistance by applying a computational fluid dynamics (CFD) simulation.

Methods: This retrospective cohort study consists of seventeen cases with two consecutive CBCT scans obtained before (T0) and after (T1) RME. Patients were divided into two groups with respect to patency of the nasopharyngeal airway as expressed in the adenoidal nasopharyngeal ratio (AN): group 1 was comprised of patients with an AN ratio < 0.6 and group 2 encompassing those with an AN ratio ≥ 0.6 . CFD simulation at inspiration and expiration were performed based on the three - dimensional (3D) models of the UA segmented from the CBCT images. The aerodynamic characteristics in terms of pressure drop, midsagittal maximum velocity, and maximum wall shear stress were compared by independent samples t-test between the two groups at T0 and T1.

Results: At T0, the pressure drop at expiration was significantly higher in group 2 compared to group 1, whereas the difference between the two groups was not significant at T1. The midsagittal maximum velocity of the two groups decreased to some extent at expiration, but without significant difference. The midsagittal maximum velocity of group 2 was at inspiration significantly higher than that of group 1 at T0 and T1.

Conclusion: RME had a positive effect on UA airflow resistance in patients with an AN ratio ≥ 0.6 . The findings provide positive evidence of RME in airway function and should thus be recommended to patients with both a narrow maxilla and enlarged adenoid.

Background

Adenoid hypertrophy (AH) is a common cause of upper airway (UA) obstruction in children and adolescents. Considerable variation in AH prevalence, ranging from 27–80%, has been reported between countries and ages [1]. AH may cause several health issues including mouth breathing, snoring, asthma, speech problems, and obstructive sleep apnoea [2, 3]. To diagnose the degree of AH, Fujioka proposed calculating an adenoidal nasopharyngeal (AN) ratio by measuring adenoid thickness and nasopharyngeal width on lateral radiography, a common procedure in clinics [4, 5]. An AN ratio of more than 0.6 indicates a suspected nasal obstruction [2]. Otolaryngologists usually suggest an adenoidectomy to treat severe nasal obstruction, and this has been shown to positively affect volume expansion in the nasopharynx and improve nasal breathing. However, a noticeable recurrence of nasal obstruction after adenoidectomy has been reported [6]. In order to achieve a stable outcome after an adenoidectomy, several adjunctive treatments have been suggested for patients with specific symptoms including turbinoplasty, adenotonsillectomy, and rapid maxillary expansion (RME) [7–9].

AH may cause abnormal craniofacial development such as a short cranial base, long face, small and narrow maxilla, and mandibular retrusion [10–12]. Some orthodontists suggest that RME may have the potential to reduce nasal obstruction by opening the midsagittal suture, widening the maxillary arch, and increasing nasal space [9, 13, 14].

RME's possible effect on nasal obstruction has been evaluated by several methods including rhinomanometry, acoustic rhinometry, polysomnography (PSG), cephalometric radiographs, cone beam computed tomography (CBCT) and computed tomography (CT), but with an inconsistent conclusions[15, 16]. Laboratory-based PSG is considered the gold standard for diagnosing obstructive sleep apnoea, as it provides quantitative parameters to evaluate respiratory function such as the apnoea-hypopnea index [17]. However, it also has limited availability and is relatively expensive and time-consuming, which could be inconvenient for children and their families. Therefore, researchers have been searching for alternative methods to evaluate the respiratory function of UA. For example, De Backer et al.[18] introduced computational fluid dynamics (CFD) as a diagnostic tool to observe the outcome of mandibular advancement devices when treating sleep-related breathing disorders and found that CFD models precisely capture UA's aerodynamic characteristics. Moreover, the CFD results show a higher correlation with clinical symptoms than volumetric measurements on CT images.

The CFD method is a well-established technique that has been widely used in mechanical engineering, yet it is quite new to flow analysis in medicine. Based on a three-dimensional (3D) structure segmented from CBCT, CT, or magnetic resonance imaging (MRI), the CFD simulates and calculates the flow of gases or fluids and their interactions with the surrounding surfaces as defined by boundary conditions. At a given inlet pressure, the shape and boundary condition of a pipe-like upper airway would theoretically determine the aerodynamic characteristics in terms of pressure, velocity, and wall shear stress. The application of CFD in dentistry is nevertheless sparse. Few previous studies have shown that CFD could be applied to evaluate the outcome of mandible advanced devices on respiratory function [18–20]. Regarding the effect of RME on airflow within the UA, Iwasaki et al. observed an improvement in nasal cavity obstruction [21] and a decrease in pharyngeal airway pressure after RME [22]. More clinical evidence on the changes of UA following RME is, however, needed to enhance and benefit individual treatment planning for patients with a narrow maxilla and enlarged adenoid.

In this study, we aim to evaluate the effect of RME on airflow within the UA by investigating the aerodynamic characteristics that result from applying CFD simulation. The hypothesis is that RME has a positive effect on UA ventilation.

Methods

This is a retrospective cohort study. All methods were carried out in accordance with the declaration of research involving human subjects and the regional ethical and scientific guidelines in vestland region, Norway. Data for all patients who had undergone RME were retrospectively collected at the Department of Orthodontics (Stomatological hospital, Dalian, China) between January 2013 and December 2016. The inclusion criteria were patients younger than 15 years old who had both pre- and post- CBCT scans due to orthodontic indication. The pre-RME CBCTs were taken within seven days prior to fixing the expander (T0) and the post-RME CBCTs at the removal of expanders (T1). The exclusion criteria were severe abnormalities of maxillofacial tissue, previous surgery on skeletal and soft tissue related to respiration, and previous orthodontic or orthopaedic treatment. Eventually, 17 patients (mean age 12 years, 11 male/6 female) were eligible for inclusion in the study. An experienced radiologist viewed all CBCT scans and ensured that the images were qualified to construct 3D models of the upper airway.

RME

A fixed Hyrax expander was used for RME, banded to the maxillary first premolars and first molars. The patient, or their guardian, rotated the expansion screw twice a day at home and a clinical check-up was performed by orthodontists once a week. After achieving the desired expansion, the expander remained in place for at least three months to stabilise the expansion.

CFD simulation

Figure 1 demonstrates the stepwise procedure of the CFD modelling and simulation, including 3D segmentation, mesh generation, and aerodynamic results.

CBCT imaging

The examination protocol of CBCT scans was as follows: field of view (FOV) 16x13 cm; tube potential 120 kVp and tube current 5 mA; scanning time 14.7 seconds (3D eXam; KaVo, Biberach an der Riss, Germany). The voxel size was set at 0.2 mm, and the contrast resolution had a 14-bit depth. All CBCT examinations were performed according to the standardised clinical routine, i.e. with the Frankfort horizontal plane parallel to the floor, teeth in maximum intercuspation, and peaceful nasal breathing without swallowing. We divided the patients into two groups according to the AN ratio at baseline (T0): group 1 was comprised of individuals with an AN ratio < 0.6 and group 2 encompassing those with an AN ratio ≥ 0.6 . The CBCT images were imported to MIMICS software (MIMICS, Materialise, Belgium) in the digital imaging and communications in medicine (DICOM) format for later analysis. To segment the 3D UA, one author (XF) orientated the CBCT image. An appropriate threshold was set from -1024 to -500 to involve the UA without deflection, which was called a "mask". The superior boundary was defined on the mask as perpendicular to the horizontal plane through the most posterior point of middle turbinate in the sagittal view; the inferior boundary was parallel the horizontal plane through the most anterior-inferior point of cervical vertebra 4. The 3D UA was then calculated from the defined mask. The superior and inferior boundaries were extended by 20mm to avoid flow reversing [23]. The extended 3D model was used to create a surface model for further mesh generation.

Mesh generation

Mesh generation is the practice of creating a mesh by computer algorithms. The continuous geometric UA space may be subdivided into discrete geometric cells. Mesh cell is the fundamental element of the reconstructed space that contains a local approximation of aerodynamic characteristics, which will be used for a later calculation. We chose tetrahedral and prismatic cells to construct the main body and boundary layer of the UA (ANSYS, Inc., Canonsburg, Pennsylvania). Each UA mesh had five boundary layers and an average of 2 million elements. The inlet and outlet of UA were defined at the extended superior and inferior boundary, as earlier described.

Aerodynamic analysis

ANSYS Fluent (ANSYS, Inc.) was applied to simulate the airflow of UA, and the SST κ - ω model was used to calculate the aerodynamic characteristics of UA. The wall of UA was defined as no-slip, stationary, and rigid, and the temperature and density of air were set as fixed [24]. In the inspiratory phase, the inlet was set with

pressure 0 Pa and the outlet a flow rate of - 200 mL/s [21]. The corresponding values were - 200 mL/s and 0 Pa at inlet and outlet for the expiratory phase. Over 2000 iterations were performed to ensure the resulting residuals were less than 10^{-6} . A radiologist (XF) performed all the simulations under the technical supervision of an engineer (YCC).

Data Analyses

We calculated the aerodynamic characteristics at inspiratory and expiratory phases, including mean pressure at the four planes defined on UA (Fig. 2). The parameters included are the pressure drop from plane 1 to plane 4, the maximum velocity of the midsagittal slice, and maximum wall shear stress at T0 and T1. Data were processed using the Statistical Package for the Social Sciences (SPSS Statistics, version 25.0, IBM, New York, NY, USA). Significance was set at p less than 0.05. Independent samples t-test was used to compare the differences of the aerodynamic characteristics between the two groups at T0 and T1.

Results

The comparison of aerodynamic characteristics in terms of pressure drop, midsagittal maximum velocity and maximum wall shear stress of the UA between the two groups before (T0) and after (T1) RME were shown in Table 1.

Table 1. Pressure drop, midsagittal-maximum velocity, and maximum wall shear stress at inspiration and expiration before (T0) and after (T1) rapid maxillary expansion, and comparison between group 1 (n=10) and group 2 (n=7)

	T0				T1					
	group 1	group 2				group 1	group 2			
	Mean	SD	Mean	SD	P value	Mean	SD	Mean	SD	P value
Inspiration										
Pressure drop	-3.700	1.800	-4.431	2.026	0.447	-3.827	2.249	-5.110	2.696	0.303
Midsagittal-maximum velocity	2.190	0.508	2.903	0.755	0.034*	2.054	0.483	2.958	1.157	0.041*
Maximum wall shear stress	1.660	1.481	0.759	0.513	0.146	0.690	0.510	1.523	1.948	0.211
Expiration										
Pressure drop	1.952	2.496	4.402	2.006	0.048*	2.032	2.230	3.934	2.412	0.115
Midsagittal-maximum velocity	2.636	1.186	3.004	0.978	0.509	2.044	0.566	2.616	1.050	0.166
Maximum wall shear stress	2.169	2.276	0.861	0.391	0.157	0.713	0.610	1.249	0.777	0.132

Inspiratory phase

Group 2 exhibited a significantly higher midsagittal maximum velocity compared to group 1 at T0 ($p = 0.034$). This may indicate that the relatively contracted region of UA was narrower in group 2 than in group 1. The difference between the two groups remained significant at T1 ($p = 0.041$) during the inspiratory phase.

The pressure drop and maximum wall shear stress were not significantly different between the two groups at T0 and T1.

Expiratory phase

During the expiratory phase, the pressure drop at T0 was significantly higher in group 2 than in group 1 ($p = 0.048$), whereas the two groups showed no significant difference in terms of pressure drop ($p = 0.115$) at T1. Figure 3 illustrates the difference in pressure drop between the two groups by presenting the mean pressure at the defined four planes of the UA.

There was no significant difference in midsagittal maximum velocity and maximum wall shear stress between the two groups at T0 and T1, respectively.

Discussion

CFD simulation

In this study, CFD simulation was applied to demonstrate the aerodynamic characteristics of the UA in patients with normal and enlarged adenoids before and after RME. The pressure drop between plane one and plane four within the UA was significantly higher in group 2 compared to group 1 (4.402 vs 1.952) during expiration at T0. This finding was in agreement with a previous study, where patients with the obstructive sleeping problem had a higher pressure drop during the expiratory phase than the healthy subjects [25]. In the engineering field, the pressure drop is defined as the pressure difference between two points of a fluid carrying network, which occurs when **frictional** forces, caused by the resistance to flow, interact with **fluid** as it flows through the tube. Applying this concept to airflow passing through the UA, the pressure drop occurs when the physiologic force is caused by morphologic changes in the UA. Previous studies found that the airflow resistance at expiration was closely related to obstruction severity in patients with obstructive sleep apnoea symptoms [26, 27]. The phenomenon may be explained by the fact that the respiratory muscles typically relax at the end of expiration; in addition, the airflows situate at the narrow, superior part of the UA, resulting in a higher risk of airway collapse [26].

Our results show that the pressure drop was reduced after RME, most prominently in group 2 at expiration, which illustrates the positive effect of RME on the improvement of respiratory function. With the same pre RME volume of airflow, the decrease pressure drop indicates the reduced airflow resistance after RME. A similar result was reported by Iwasaki et al.[22], where the authors found that the nasal resistance at expiration significantly decreased in the nasal cavity after RME.

In line with the changes in pressure drop post RME, we observed a decrease in the velocity of airflow at the expiratory phase in group 2. This trend was supported by the results of Faramarzi et al., who evaluated the aerodynamics of the nasal cavity in a patient with septal perforation and found that velocity was higher in the area that showed a higher pressure drop [28]. In our study, we failed to observe any statistically significant change in terms of maximum wall shear stress between either T0 and T1 or the two groups. This may indicate that the changes in airflow were not significant enough to be recognised in terms of maximum wall shear stress.

CFD is a valuable tool for investigating the aerodynamic characteristics of the UA; more functional characteristics could be obtained from CFD models in contrast to the solely morphological characteristics derived from 3D models. In an unpublished study on the same group of patients (study submitted), we observed a non-significant tendency of volumetric increase in the nasopharyngeal airway in group 2 after RME. Furthermore, after applying CFD simulation, the present study also shows significant changes in terms of pressure drop in group 2 after RME. A similar finding was reported by Iwasaki, in which CFD simulation was preferred to 3D geometric measurements in detecting nasal cavity obstruction [21]. Based on the present study, the most sensitively altered parameter after RME was the pressure drop, i.e. the pressure variation at different levels in the UA. The pressure drop seems to be a feasible parameter to represent the airflow resistance, and the concept may be readily accepted by clinicians.

At present, the simulation procedure is not entirely automatic and thus very time-consuming. Part of the 3D segmentation and mesh generation needs to be performed manually due to the irregular anatomic structure of the UA. It may be possible to improve and shorten the simulating process in the future with the development of artificial intelligence.

Clinical implications

The CFD method makes the aerodynamic characteristics within the UA visible. We found that after RME the decrease in pressure drop was more pronounced in group 2 during expiration, which provided quantitative evidence to support the positive effect of RME on UA ventilation. This indicates that RME could be a beneficial method to reduce airflow resistance, especially for patients with enlarged adenoids. Due to the intrinsic nature of a retrospective study design, the lack of clinical otolaryngologic examination makes it difficult to conclude whether RME alone would be sufficient for the treatment of nasal obstruction caused by an enlarged adenoid. Nevertheless, RME may be recommended for patients who have a narrow maxilla and enlarged adenoid. Further randomized control study is warranted to investigate whether RME shall be combined with the adenoidectomy to enhance the treatment outcome.

Conclusions

Our findings demonstrate the positive effect of RME on airflow in patients with enlarged adenoids by analysing aerodynamic characteristics, which indicates that RME may be a beneficial method to decrease airflow resistance for patients with enlarged adenoids.

Declarations

Ethics approval and consent to participate

The study was approved by the ethics committee of China (DLKQLL201604, Dalian Stomatological Hospital) as well as the ethics committee of Norway (2018/1547 REK Vest, University of Bergen). Written informed consent was obtained from all participants or their legal guardians.

Consent for publication

Not applicable as there are no participants' identifiable data, picture or illustrations that require consent to publish in this manuscript.

Availability of data and materials

All data used and/or analysed during the current study are available from the corresponding author on reasonable request.

Competing interests

The authors declare that they have no competing interest.

Funding

This work was supported by grants provided by Dalian Medical Science Project, China (No. 1611079) as well as grants provided by University of Bergen, Norway (SPIRE project). The funding body was not involved in the study design, data collection, data analysis, or interpretation of data, or in writing the manuscript.

Author's contributions

X. Feng contributed to design, data acquisition, image segmentation, CFD simulation, and interpretation, drafted and critically revised the manuscript. Y.C. Chen contributed to the study design and supervised the CFD simulation process. K. Hellén-Halme contributed to conception, design, and supervised manuscript writing. W.H.Cai contributed to conception and design with respect to CFD simulation. X-Q Shi contributed to conception, design, data interpretation, and critically revised the manuscript. All authors commented on all drafts of the manuscript. All authors read and approved the final manuscript.

Acknowledgements

Not applicable

References

1. Pereira L, Monyror J, Almeida FT, Almeida FR, Guerra E, Flores-Mir C, Pacheco-Pereira C: Prevalence of adenoid hypertrophy: A systematic review and meta-analysis. *Sleep Med Rev* 2018, 38:101–112.
2. Tatlipinar A, Biteker M, Meric K, Bayraktar GI, Tekkesin AI, Gokceer T: Adenotonsillar hypertrophy: correlation between obstruction types and cardiopulmonary complications. *Laryngoscope* 2012, 122(3):676–680.
3. Pagella F, De Amici M, Pusateri A, Tinelli G, Matti E, Benazzo M, Licari A, Nigrisoli S, Quaglini S, Ciprandi G *et al*: Adenoids and clinical symptoms: Epidemiology of a cohort of 795 pediatric patients. *Int J Pediatr Otorhinolaryngol* 2015, 79(12):2137–2141.
4. Fujioka M, Young LW, Girdany BR: Radiographic evaluation of adenoidal size in children: adenoidal-nasopharyngeal ratio. *AJR American journal of roentgenology* 1979, 133(3):401–404.
5. Duan H, Xia L, He W, Lin Y, Lu Z, Lan Q: Accuracy of lateral cephalogram for diagnosis of adenoid hypertrophy and posterior upper airway obstruction: A meta-analysis. *Int J Pediatr Otorhinolaryngol* 2019, 119:1–9.
6. Mitchell RB, Archer SM, Ishman SL, Rosenfeld RM, Coles S, Finestone SA, Friedman NR, Giordano T, Hildrew DM, Kim TW *et al*: Clinical Practice Guideline: Tonsillectomy in Children (Update). *Otolaryngology–head and neck surgery: official journal of American Academy of Otolaryngology-Head and Neck Surgery* 2019, 160(1_suppl):S1-S42.
7. Chohan A, Lal A, Chohan K, Chakravarti A, Gomber S: Systematic review and meta-analysis of randomized controlled trials on the role of mometasone in adenoid hypertrophy in children. *Int J Pediatr Otorhinolaryngol* 2015, 79(10):1599–1608.
8. Baik G, Brietzke SE: Cost Benefit and Utility Decision Analysis of Turbinoplasty with Adenotonsillectomy for Pediatric Sleep-Disordered Breathing. *Otolaryngology–head and neck surgery: official journal of American Academy of Otolaryngology-Head and Neck Surgery* 2019, 161(2):343–347.

9. Guillemineault C, Monteyrol PJ, Huynh NT, Pirelli P, Quo S, Li K: Adeno-tonsillectomy and rapid maxillary distraction in pre-pubertal children, a pilot study. *Sleep Breath* 2011, 15(2):173–177.
10. Schendel SA, Eisenfeld J, Bell WH, Epker BN, Mishelevich DJ: The long face syndrome: vertical maxillary excess. *American journal of orthodontics* 1976, 70(4):398–408.
11. Macari AT, Bitar MA, Ghafari JG: New insights on age-related association between nasopharyngeal airway clearance and facial morphology. *Orthod Craniofac Res* 2012, 15(3):188–197.
12. Garetz SL, Mitchell RB, Parker PD, Moore RH, Rosen CL, Giordani B, Muzumdar H, Paruthi S, Elden L, Willging P *et al*: Quality of life and obstructive sleep apnea symptoms after pediatric adenotonsillectomy. *Pediatrics* 2015, 135(2):e477-486.
13. Huynh NT, Desplats E, Almeida FR: Orthodontics treatments for managing obstructive sleep apnea syndrome in children: A systematic review and meta-analysis. *Sleep Med Rev* 2016, 25:84–94.
14. Hamoda MM, Kohzuka Y, Almeida FR: Oral Appliances for the Management of OSA: An Updated Review of the Literature. *Chest* 2018, 153(2):544–553.
15. Di Carlo G, Saccucci M, Ierardo G, Luzzi V, Occasi F, Zicari AM, Duse M, Polimeni A: Rapid Maxillary Expansion and Upper Airway Morphology: A Systematic Review on the Role of Cone Beam Computed Tomography. *BioMed research international* 2017, 2017:5460429.
16. Kilic N, Oktay H: Effects of rapid maxillary expansion on nasal breathing and some naso-respiratory and breathing problems in growing children: a literature review. *Int J Pediatr Otorhinolaryngol* 2008, 72(11):1595–1601.
17. Roland PS, Rosenfeld RM, Brooks LJ, Friedman NR, Jones J, Kim TW, Kuhar S, Mitchell RB, Seidman MD, Sheldon SH *et al*: Clinical practice guideline: Polysomnography for sleep-disordered breathing prior to tonsillectomy in children. *Otolaryngology–head and neck surgery: official journal of American Academy of Otolaryngology-Head and Neck Surgery* 2011, 145(1 Suppl):S1-15.
18. De Backer JW, Vanderveken OM, Vos WG, Devolder A, Verhulst SL, Verbraecken JA, Parizel PM, Braem MJ, Van de Heyning PH, De Backer WA: Functional imaging using computational fluid dynamics to predict treatment success of mandibular advancement devices in sleep-disordered breathing. *J Biomech* 2007, 40(16):3708–3714.
19. Zhao M, Barber T, Cistulli P, Sutherland K, Rosengarten G: Computational fluid dynamics for the assessment of upper airway response to oral appliance treatment in obstructive sleep apnea. *J Biomech* 2013, 46(1):142–150.
20. Martínez A, Muñoz AL, Soudah E, Calvo J, Suárez AÁ, Cobo J, Cobo T: Physiological and geometrical effects in the upper airways with and without mandibular advance device for sleep apnea treatment. *Scientific reports* 2020, 10(1):5322–5322.
21. Iwasaki T, Saitoh I, Takemoto Y, Inada E, Kanomi R, Hayasaki H, Yamasaki Y: Improvement of nasal airway ventilation after rapid maxillary expansion evaluated with computational fluid dynamics. *Am J Orthod Dentofacial Orthop* 2012, 141(3):269–278.
22. Iwasaki T, Takemoto Y, Inada E, Sato H, Suga H, Saitoh I, Kakuno E, Kanomi R, Yamasaki Y: The effect of rapid maxillary expansion on pharyngeal airway pressure during inspiration evaluated using computational fluid dynamics. *Int J Pediatr Otorhinolaryngol* 2014, 78(8):1258–1264.

23. Cisonni J, Lucey AD, King AJ, Islam SM, Lewis R, Goonewardene MS: Numerical simulation of pharyngeal airflow applied to obstructive sleep apnea: effect of the nasal cavity in anatomically accurate airway models. *Med Biol Eng Comput* 2015, 53(11):1129–1139.
24. Powell NB, Mihaescu M, Mylavarapu G, Weaver EM, Guilleminault C, Gutmark E: Patterns in pharyngeal airflow associated with sleep-disordered breathing. *Sleep Med* 2011, 12(10):966–974.
25. Chen H, Li Y, Reiber JH, de Lange J, Tu S, van der Stelt P, Lobbezoo F, Aarab G: Analyses of aerodynamic characteristics of the oropharynx applying CBCT: obstructive sleep apnea patients versus control subjects. *Dentomaxillofac Radiol* 2018, 47(2):20170238.
26. Verbraecken JA, De Backer WA: Upper airway mechanics. *Respiration* 2009, 78(2):121–133.
27. Tamisier R, Pepin JL, Wuyam B, Deschaux C, Levy P: Expiratory changes in pressure: flow ratio during sleep in patients with sleep-disordered breathing. *Sleep* 2004, 27(2):240–248.
28. Faramarzi M, Baradaranfar MH, Abouali O, Atighechi S, Ahmadi G, Farhadi P, Keshavarzian E, Behniafard N, Baradaranfar A: Numerical investigation of the flow field in realistic nasal septal perforation geometry. *Allergy Rhinol (Providence)* 2014, 5(2):70–77.

Figures

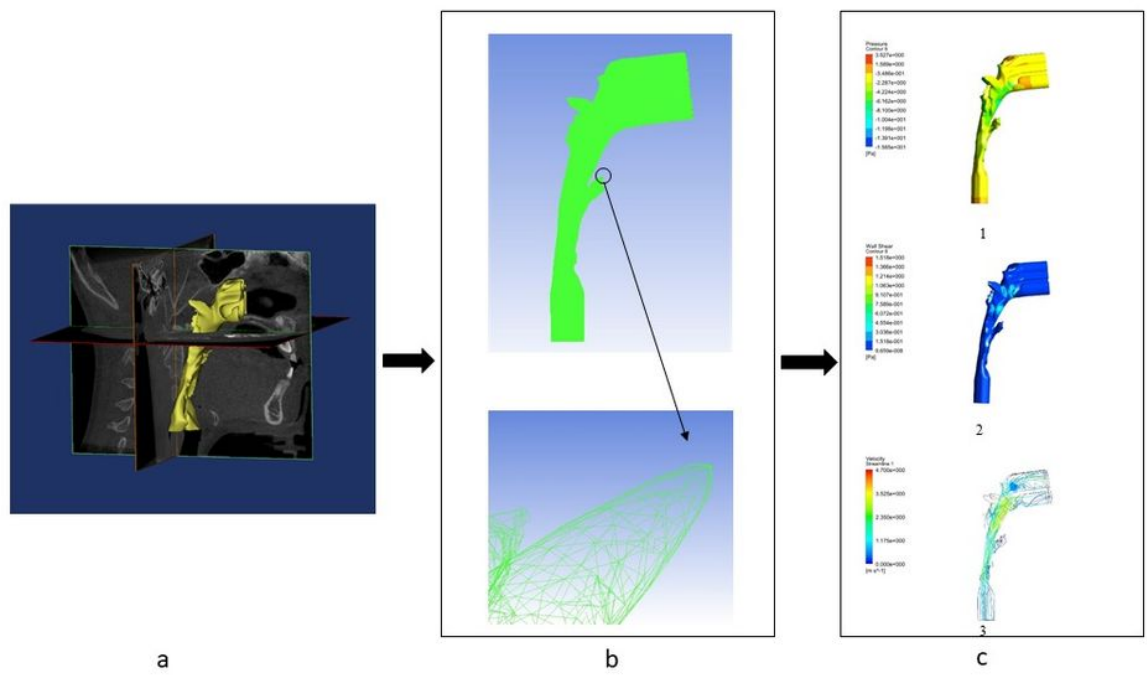


Figure 1

The procedure of CFD modeling and simulation. (a) CBCT images; (b) Mesh generation and detailed zoom; (c) Aerodynamic results: 1. airflow pressure, 2. wall shear pressure, 3. velocity.

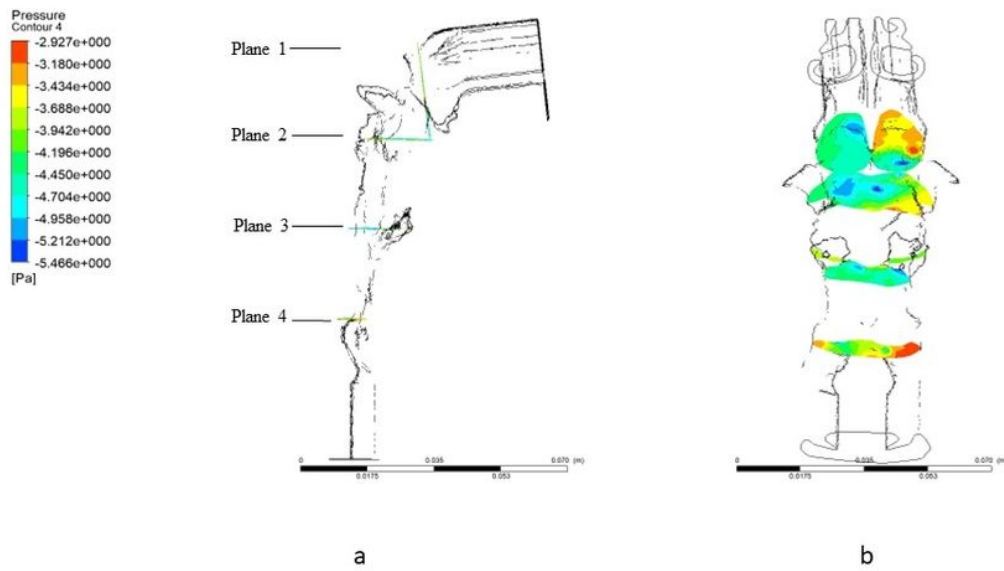


Figure 2

Description of the pressure of 4 planes defined on the CFD model (a) Definition of the four planes in the sagittal view: plane 1, paralleled the inlet plane through the posterior point of middle turbinate; plane 2, paralleled the outlet plane through the inferior point of plane 1; plane 3, paralleled the outlet plane through the tip of the soft palate; plane 4, paralleled the outlet plane through the tip of the epiglottis. (b) Distribution of the pressure of each plane in the posterior view.

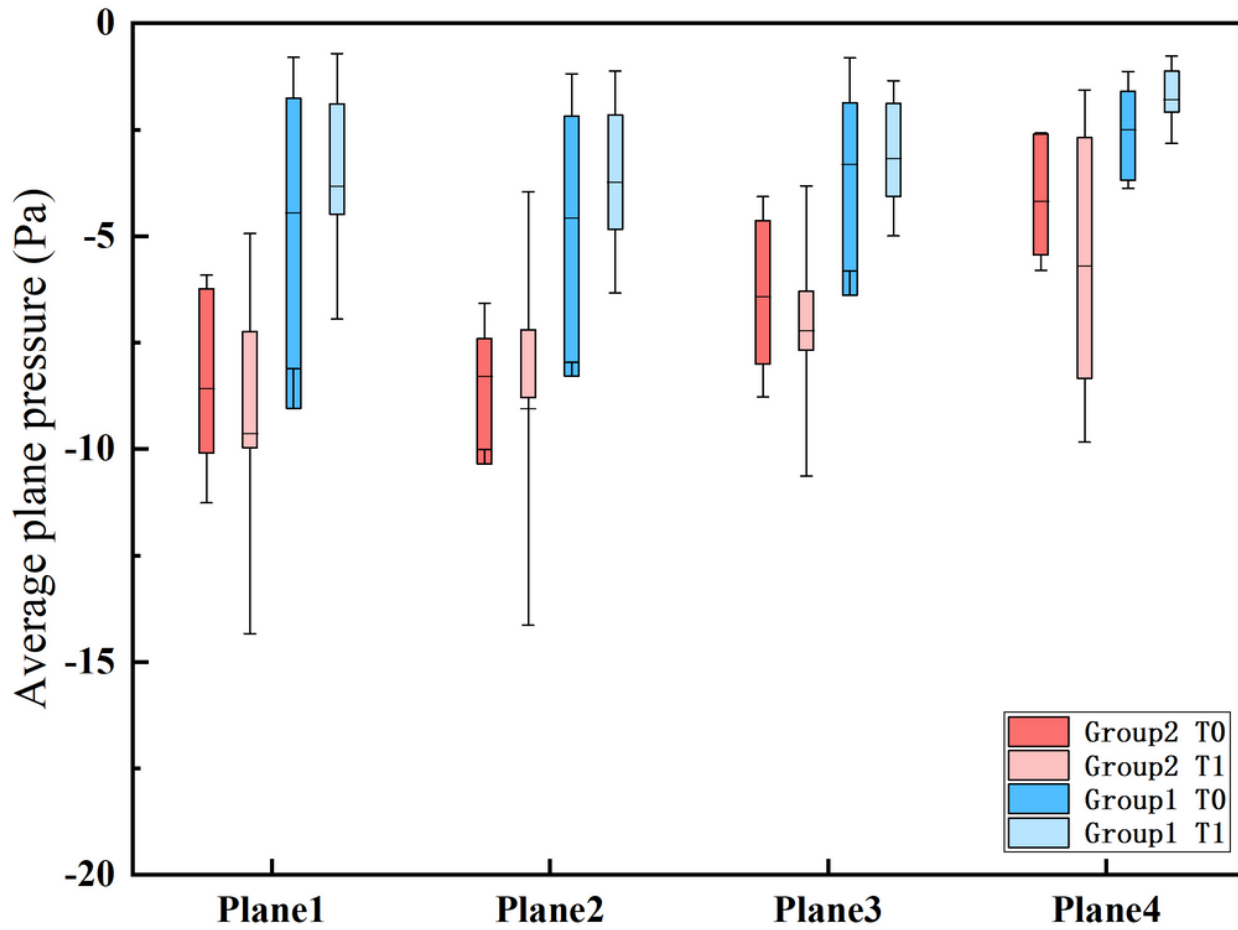


Figure 3

The mean pressure changes of the 4 planes (Mean with SD) at the expiratory phase.